NANO LETTERS

pubs.acs.org/NanoLett Letter

Topological Band Engineering of Lieb Lattice in Phthalocyanine-Based Metal−Organic Frameworks

Wei Jiang, Shunhong Zhang, Zhengfei Wang, Feng Liu,* and Tony Low*

Cite This: *Nano Lett.* 2020, 20, 1959−1966 Read Online

ACCESS | Metrics & More | Article Recommendations | Supporting Information

ABSTRACT: Topological properties of the Lieb lattice, i.e., the edge-centered square lattice, have been extensively studied and are, however, mostly based on theoretical models without identifying real material systems. Here, based on tight-binding and first-principles calculations, we demonstrate the Lieb-lattice features of the experimentally synthesized phthalocyanine-based metal−organic framework (MPc-MOF), which holds various intriguing topological phase transitions through band engineering. First, we show that the MPc-MOFs indeed have a peculiar Lieb band structure with 1/3 filling, which has been overlooked because of its unconventional band structure deviating from the ideal Lieb band. The intrinsic MPc-MOF presents a trivial insulating state, with its gap size determined by the on-site energy difference (ΔE) between the corner and edge-center sites. Through either chemical substitution or physical strain engineering, one can tune ΔE to close the gap and achieve a topological phase transition. Specifically, upon closing the gap, topological semimetallic/insulating states emerge from nonmagnetic MPc-MOFs, while magnetic semimetal/Chern insulator states arise from magnetic MPc-MOFs, respectively. Our discovery greatly enriches our understanding of the Lieb lattice and provides a guideline for experimental observation of the Lieb-lattice-based topological states.

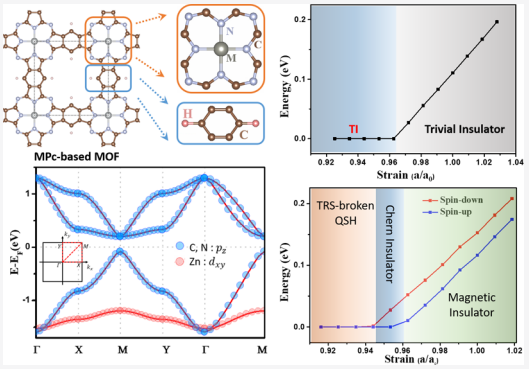

KEYWORDS: *Lieb lattice, electronic topology, metal-phthalocyanine, metal−organic framework, first-principles calculations*

INTRODUCTION

The Lieb lattice, i.e., two-dimensional (2D) edge-centered square lattice (Figure 1a), is named after American mathematical physicist, Elliott H. Lieb, for his discovery of the itinerant-electron ferromagnetism based on the Hubbard model in such a lattice decades ago.[1] Various intriguing quantum states have been proposed based on the exotic Dirac and flat bands in the presence of strongly correlated electrons, e.g., ground-state ferromagnetism, superconductivity, and topological states.[1−5] Though having been widely studied, most previous works are based on theoretical models, because real material systems with the Lieb lattice are very difficult to find. So far, the Lieb lattice has been mostly realized in artificial systems, such as using photonic, cold-atom, or surface patterning techniques.[5−8] Very recently, one experimentally synthesized 2D covalent-organic framework (COF) was identified theoretically as the distorted Lieb-lattice material with the coexistence of Lieb-3 and Lieb-5 types.[4,9,10] However, this COF-material is found to be a trivial insulator intrinsically, and it prohibits the exploration of the topological properties of the Lieb lattice because an unrealistically high doping concentration is required to reach the topological state. It is therefore of practical interest to find a real Lieb-lattice material with reachable topological states by doping and/or strain engineering.[11,12]

Based on theoretical models,[3,13−15] the nontrivial flat band due to the destructive interference in the ideal Lieb lattice requires stringent lattice symmetry and zero next-nearest-neighbor (NNN) hopping. This is very hard to be realized in real materials due to the nonvanishing wave function overlaps.[4] So far, this has only been achieved in photonic crystals, where the NNN hoppings are artificially suppressed to show the characteristic feature of the flat band by constructing a static state at the edge-center positions.[5,6] On the other hand, the topological features emerging from the Dirac cone show a certain degree of "robustness", which have less strict requirements about the lattice symmetry or hopping. Though various topological states have been proposed while modifying these factors in the Lieb lattice,[3,13,15] a clear physical picture that can guide the search is missing, which has hindered our materials discovery.

Recently, predictions of a 2D organic topological insulator and successful experimental syntheses of 2D π-conjugated metal−organic and covalent-organic frameworks (MOFs/

Received: December 20, 2019
Revised: February 15, 2020
Published: February 20, 2020

https://dx.doi.org/10.1021/acs.nanolett.9b05242
Nano Lett. 2020, 20, 1959−1966

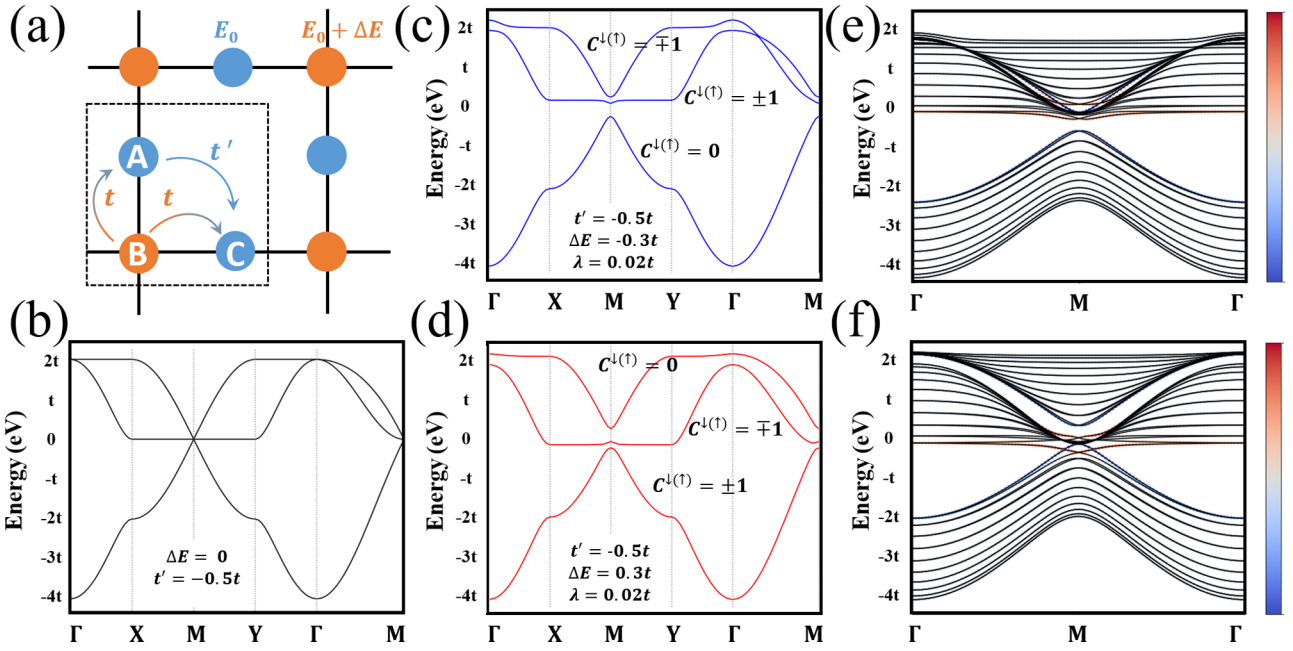

Figure 1. Tight binding model of the Lieb lattice. (a) Crystal structure of the Lieb lattice with one corner (B) and two edge-center sites (A and C), where on-site energies are E_0 and $E_0 + \Delta E$ for A/C and B, respectively. t and t' represent the NN and NNN hopping, respectively. (b) Band structure of the nonideal Lieb lattice when ΔE equals zero and t' equals $-0.5t$. (c, d) Band structure of the disturbed Lieb lattice with ($t' = -0.5t$, $\Delta E = -0.3t$, and $\lambda = 0.02t$) and ($t' = -0.5t$, $\Delta E = 0.3t$, and $\lambda = 0.02t$), respectively. We note that t is set with positive value. Spin Chern numbers for each band are labeled nearby. (e, f) Ribbon band structure for parts c and d, respectively, with red and blue colors highlighting contributions from two edges.

COFs) have triggered considerable interests in studying exotic physics in MOFs/COFs beyond their traditional applications.[16−24] With advances of the modern chemistry synthetic ability, MOFs/COFs can be grown with a designed geometry and highly crystalline quality, leading to a very high tunability and diversity, as their structure can be made with varying combinations of organic ligands and metal ions. This renders MOFs/COFs ideal platforms to realize various intriguing quantum phases, such as quantum spin Hall and fractional quantum Hall states.[22−25] For the same reason, we anticipate that Lieb-lattice materials with the predicted intrinsic/extrinsic topological properties can also be realized within this huge family of organic materials, where chemical and/or physical engineering become feasible.

In this Letter, we will first comprehensively demonstrate the Lieb lattice properties using tight-binding (TB) method, based on which the basic physical principle to realize topological states is illustrated. Then, we revisit a family of phthalocyanine-based MOFs (MPc-MOFs) in a square lattice and elaborate on the finding that the MPc-MOFs actually belong to the Lieb lattice with a nonideal Lieb band structure in a trivial insulating phase. More importantly, we show that, by applying the working physical principle we established, the trivial insulators could be tailored into topological nontrivial states, e.g., topological semimetal, topological insulator, and Chern semimetal, through chemical decoration and/or strain engineering. The topological properties are confirmed through calculations of topological invariant, edge state, and Wannier charge centers. We suggest the crystalline MPc-MOFs as the first real material system to realize the rich variants of topological Lieb lattices.

RESULTS AND DISCUSSION

Tight-Binding Model. The Lieb lattice having the D_{4h} group symmetry essentially contains one corner and two edge-center sites, which have a coordination number of four and two, respectively. Before discussing real material systems, we first illustrate the essential features of the Lieb lattice using a single orbital TB model. The corner site B and two edge-center sites A and C are shown in Figure 1a. The Hamiltonian that includes only the nearest-neighbor (NN) and next-nearest-neighbor (NNN) hoppings is written as

$$\mathcal{H}_0 = \sum_i \epsilon_i c_i^\dagger c_i + \sum_{\langle i,j\rangle} t c_i^\dagger c_j + \sum_{\langle\langle i,j\rangle\rangle} t' c_i^\dagger c_j + H.c. \quad (1)$$

where $c_i^\dagger$ and c_i are the creation and annihilation operators of an electron on the site i, respectively; t and t' represent the hopping amplitudes between the NN $\langle i, j\rangle$ and the NNN $\langle\langle i, j\rangle\rangle$ sites, respectively. ϵ_i is the on-site energy (OSE) on site i, which is set to be the same for edge-center sites, A and C. The OSE difference between B and A sites is $\Delta E = \epsilon_B - \epsilon_A$. The Lieb lattice has been studied for the ideal case by setting both t' and ΔE equal to zero, which is however unrealistic in real materials. This is because of the extensive nature of electron wave functions and the unavoidable chemical potential difference between the corner and edge-center states that lead to a nonvanishing NNN interaction and nonzero ΔE,[4] respectively.

To be more generic as in real materials, one must add two additional terms, i.e., ΔE and NNN hopping t', in the Hamiltonian. We note that ΔE and t' are scaled with t, where t is set with positive values in our model. By transforming $\mathcal{H}_0$ into momentum space using $\mathcal{H} = \sum_k \Psi_k^\dagger H(k) \Psi_k$, where $\Psi_k^\dagger = (c_{Ak}^\dagger, c_{Bk}^\dagger, c_{Ck}^\dagger)$, one obtains the matrix Hamiltonian:

https://dx.doi.org/10.1021/acs.nanolett.9b05242
Nano Lett. 2020, 20, 1959−1966

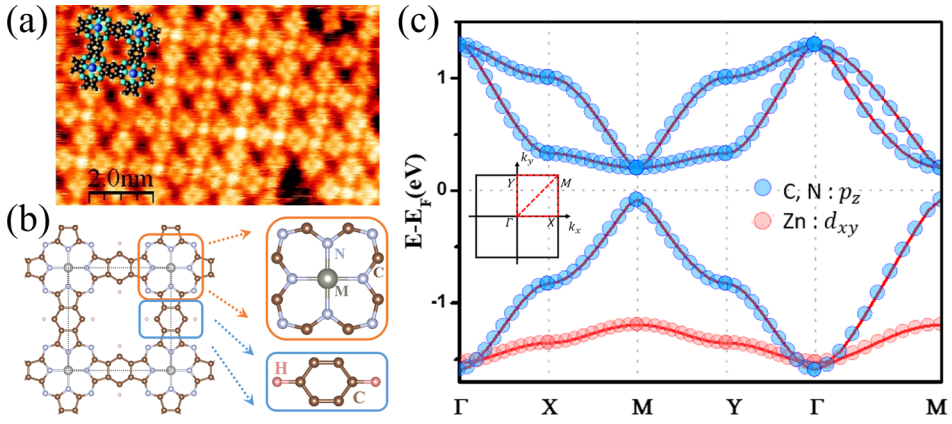

Figure 2. Phthalocyanine-based metal−organic frameworks. (a) Scanning tunneling microscopy image of experimentally synthesized MPc-MOF crystal. (b) Crystal structure of MPc-MOF, where the corner and edge-center units are highlighted in the enlarged orange and blue rectangles, respectively. (c) Band structure of ZnPc-MOF, which corresponds to the $t' = -0.5t$ and $\Delta E < 0$ scenario. The blue and red circles show the different orbital contribution to the bands around the Fermi level. The inset shows the first Brillouin zone with high-symmetry k-paths highlighted by red dashed lines. Panel a is reprinted in part with permission from ref 32. Copyright 2011 American Physical Society.

$$H(k) = \begin{pmatrix} \varepsilon_B & -2t\cos\left(\vec{k}\cdot\frac{\vec{v_1}}{2}\right) & -2t\cos\left(\vec{k}\cdot\frac{\vec{v_2}}{2}\right) \\ -2t\cos\left(\vec{k}\cdot\frac{\vec{v_1}}{2}\right) & \varepsilon_A & -4t'\cos\left(\vec{k}\cdot\frac{\vec{v_1}}{2}\right)\cos\left(\vec{k}\cdot\frac{\vec{v_2}}{2}\right) \\ -2t\cos\left(\vec{k}\cdot\frac{\vec{v_2}}{2}\right) & -4t'\cos\left(\vec{k}\cdot\frac{\vec{v_1}}{2}\right)\cos\left(\vec{k}\cdot\frac{\vec{v_2}}{2}\right) & \varepsilon_C \end{pmatrix}$$

where $\vec{v_1} = (1, 0)$ and $\vec{v_2} = (0, 1)$ are unit vectors that define the displacement vector. $\vec{k} = (k_x, k_y)$ is the reciprocal lattice k vector. For the ideal case with ϵ_i, ΔE, and t' all equal to zero, the analytical solutions of $E_1 = 0$ and $E_{2,3} = \pm 2t\sqrt{\cos^2\left(\vec{k}\cdot\frac{\vec{v_1}}{2}\right) + \cos^2\left(\vec{k}\cdot\frac{\vec{v_2}}{2}\right)}$ can be obtained, leading to a perfectly flat band in the middle of Dirac bands. With a nonzero ΔE, corresponding eigenvalues are $E_{2,3} = \left\{\epsilon_A + \epsilon_B \pm \sqrt{(\epsilon_A - \epsilon_B)^2 + 16t^2\left[\cos^2\left(\vec{k}\cdot\frac{\vec{v_1}}{2}\right) + \cos^2\left(\vec{k}\cdot\frac{\vec{v_2}}{2}\right)\right]}\right\}/2$ and $E_1 = \epsilon_A$. It can be seen that an energy gap opens between the two Dirac bands ($|E_2 - E_3| \neq 0$), with a global gap of exactly ΔE at the M point (Supporting Information). The flat band is now only in contact with either top or bottom Dirac band at the M point, depending on the sign of ΔE.

On the other hand, for the case with a nonzero NNN interaction t' and zero ΔE, the H_{AC} term, $-4t'\cos\left(\vec{k}\cdot\frac{\vec{v_1}}{2}\right)\cos\left(\vec{k}\cdot\frac{\vec{v_2}}{2}\right)$, equals zero when k_x or $k_y = \pi/2$. Consequently, the band structure along $M - X/Y$ k-paths (boundary of the 1st Brillouin zone) is immune to the NNN interaction and remains the same as the $t' = 0$ case, as can be seen in Figure 1b. For the other k-points, the flat band will become dispersive, while the two Dirac bands will respond differently to the NNN hopping; i.e., one band will become more dispersive while the other becomes less dispersive. Specially, when $t' = -0.5t$, the middle band touches the top Dirac band at the Γ point, as can be seen in Figure 1b. It is interesting to mention that the top Dirac band becomes flat along $\Gamma - X/Y$ k-paths (Supporting Information). This can be further confirmed from the analytical solutions along these k-paths, i.e., $E_1 = 2t$; $E_{2,3} = -t\left(1 \pm \sqrt{1 + 8\cos^2\left(\vec{k}\cdot\frac{\vec{v_{1,2}}}{2}\right)}\right)$.

When considering both parameters, though analytical solutions across the whole Brillouin zone become complicated, the results at the M point ($E_1 = \epsilon_B$, $E_{2,3} = \epsilon_A = \epsilon_B + \Delta E$) and along the $M - X/Y$ remain unchanged. We find that the topological features of the Lieb lattice are mainly related to the peculiar band structure near the M point, where the band touching happens. This can be confirmed by calculating topological invariant based on the Kubo formula[26,27] and TB ribbon calculation with the inclusion of the NNN spin−orbit coupling (SOC) interaction:

$$\mathcal{H}_{soc} = i\lambda \sum_{\langle\langle i,j\rangle\rangle} v_{ij} c_i^\dagger \sigma_z c_j + H.C. \quad (2)$$

where λ describes the SOC strength; σ_z is the Pauli matrix; $v_{ij} = d_{ij}^1 \times d_{ij}^2$ with d_{ij}^1 and d_{ij}^2 represent the two NN bond vectors connecting i and j sites. Taking the Lieb lattice with 1/3 filling and $t' = -0.5t$ (t is positive) as an example, we show that when $\Delta E < 0$, the lower Dirac band is isolated from other bands, and the system is a trivial insulator, as confirmed by spin Chern number and the ribbon band structure in Figure 1c,e, respectively. When $\Delta E > 0$, the lower Dirac band is in contact

https://dx.doi.org/10.1021/acs.nanolett.9b05242
Nano Lett. 2020, 20, 1959−1966

with the middle band at the M point, which becomes gapped after considering SOC, and hence, the system changes to a topological insulator state (Figure 1d,f). Therefore, in principle, topological states can be achieved by simply manipulating energy states at the M point, which is mainly determined by ΔE. In other words, one could tune the on-site energy difference between the corner and edge-center sites to achieve topological transitions.

MPc-MOFs with a Hidden Lieb Lattice. To find real materials with topological properties hosted by a Lieb lattice, we focus our attention on the MOFs/COFs having square lattice geometry. Based on the above analyses, materials are not required to be strictly ideal with a flat band throughout the Brillouin zone and triple degeneracy at the M point. There are a few 4-fold-coordinated organic ligands that have been studied in both the chemistry and physics community. One of the most widely studied systems is the metal-phthalocyanine (MPc) family, which is famous for its potential application in molecular spintronics.[28−31] Several MPc-based crystals (MPc-MOFs) have been experimentally synthesized and theoretically studied, as shown in Figure 2a, which focused on their magnetic properties[32−34] without realizing their possible relation to the Lieb lattice and the corresponding topological properties. Here, we reveal that these experimentally synthesized MPc-MOFs actually represent an interesting family of Lieb-lattice materials with nonideal Lieb bands.

First, from the experimental scanning tunneling microscopy (STM) results in Figure 2a,[32] one can see clearly the typical Lieb-lattice feature with the corner and edge-center states in a square lattice. By further analyzing the crystalline structure of MPc-MOF in Figure 2b, the corner sites are occupied by the MPc ligand while the edge-center sites are occupied by the benzene ring. There are two "characteristic" electrons in the system that are critical for understanding its electronic and magnetic properties, i.e., localized d electrons from transition metal ions (M) that contribute to the magnetic properties, and itinerant π electrons from Pc and benzene molecules that construct the Lieb lattice and its resulting Lieb physics. The metal ions prefer the valence state of M^{2+} by donating two electrons to four coordinated N atoms due to the square-crystal-field induced d-orbital splitting. Given the crystal field splitting and exchange coupling effect, the magnetic properties of the MPc molecule and MPc-MOF crystal are well understood.[33]

A Lieb-lattice structure should, in principle, produce Lieb-lattice electronic structures. Therefore, we performed first-principles calculations on one representative material, nonmagnetic ZnPc, to confirm this hypothesis. The band structure is shown in Figure 2c, which contains four bands around the Fermi level with a noticeable band gap (≈0.35eV). From the atom- and orbital-resolved projected band structure analysis (Figure 2c), one can see there are three bands formed by the p_z orbitals of C and N atoms (blue circles) and one band below the Fermi level formed by the Zn d_{xy} orbital (red circles). Indeed, the three p_z bands look very similar to the distorted Lieb lattice in our TB model (Figure 1c). The Γ-point degeneracy and large dispersion of the middle "flat band" indicate that there is a strong NNN hopping (t') between the edge-center sites. This can be further confirmed by plotting the band-resolved partial charge distribution for these three bands (Figure 3a−c), which show a strong π-conjugation among the whole lattice with the corner and edge-center molecular orbitals highlighted by red and blue rectangles, respectively.

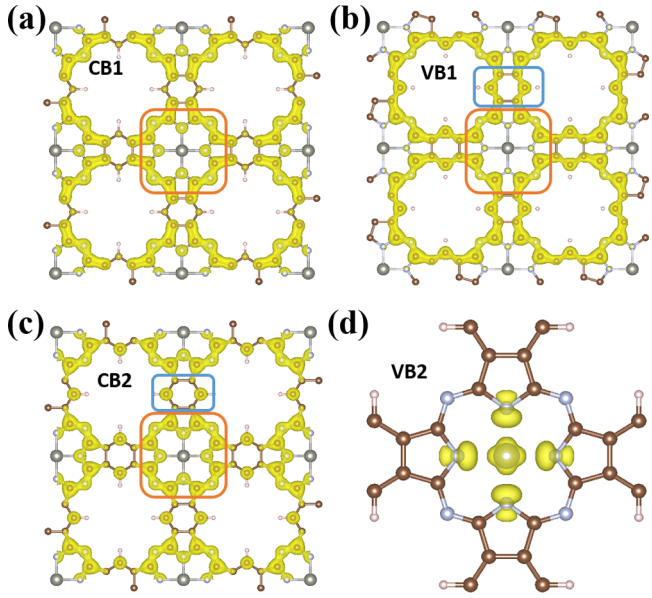

Figure 3. Band-resolved partial charge distribution. (a) Partial charge distribution for the first conduction band (CB1). (b−d) Same as part a for the first valence band (VB1), second conduction band (CB2), and second valence band (VB2), respectively. VB1, VB2, and CB1 show full π-conjugation, where the Lieb lattice is formed by the corner and edge-center site molecular orbitals as highlighted in red and blue squares, respectively. CB2 shows the localized d_{xy} orbitals of Zn.

The partial charge density for the band below shows high localization of the Zn d_{xy} orbital (Figure 3d), which is also consistent with the d^{10} electronic configuration of the Zn^{2+} under the square crystal field effect.

Having identified the hidden Lieb lattice in the MPc-MOF, next, we look into their topological properties. The Fermi level locates right in the gap between the bottom Dirac band and the middle band (Figure 2c), indicating that the Lieb system is 1/3 filled, and the OSE of the corner site is lower than that of the edge-center site. The system is therefore a topologically trivial insulator, as demonstrated in Figure 1c,e. It is of both scientific and technological interest to realize topologically nontrivial states in topological trivial materials. Our TB model analysis shows that a topological transition can be achieved by reversing the OSE difference between the corner and edge-center sites in the Lieb lattice, i.e., increase the OSE of corner state and/or decrease the OSE of edge-center states. The OSE essentially represents the local chemical potential of these states.[4] As the electronic Lieb features are only determined by the p_z electrons of the C and N elements, we can tailor the local chemical potential of the corner and edge-center states through either chemical substitution or physical strain engineering.

Practically, we propose three approaches to realize this inversion/transition: (i) increase the OSE of the corner site by replacing the central metal with metals having lower electron ionization energy; (ii) decrease the OSE of the edge-center site by decorating the benzene ring with a strong electron negativity unit, e.g., replacing H with halogen F; and (iii) vary the OSE difference by applying biaxial strain. The first two approaches could be possibly applied experimentally by using different organic ligands as the building unit. The third method is also possible by either choosing a suitable substrate for self-

https://dx.doi.org/10.1021/acs.nanolett.9b05242
Nano Lett. 2020, 20, 1959−1966

assembly or applying external strain through flexible substrates, as validated for various 2D materials.[35]

Next, through first-principles calculations, we demonstrate the aforementioned three approaches one-by-one. In general, metal ions with lower electron ionization energy have a higher tendency to donate valence electrons and, therefore, tend to increase the local chemical potential of the MPc ligands. To confirm this conjecture, we selected four elements with different ionization energies without spin polarization, i.e., Mg, Ca, Ni, and Zn. The results are summarized in Table 1,

Table 1. Band Gap for Different MPc-MOFs

materials	CaPc-MOF	MgPc-MOF	ZnPc-MOF	NiPc-MOF
ionization energy (kJ/mol)	1735.28	2188.43	2639.70	2490.17
band gap (eV)	0.047	0.073	0.110	0.216

which indeed show that the lower ionization energy of the metal ions, the smaller the band gap of the MPc-MOF crystal; e.g., the Ca with the lowest ionization energy produces the smallest gap in the CaPc-MOF. The anomalous behavior of the NiPc-MOF could be possibly due to hybridization of d states of the conduction bands (Supporting Information). On the other hand, one can lower the local potential of the edge-center states by substituting H element with elements that have higher electronegativity, which have a higher tendency to attract electrons, such as Br, Cl, and F. To confirm this hypothesis, we performed calculations based on ZnPc-MOF. The results in Table 2 show that the gap size is smaller for the element with higher electron negativity. Similar anomalous behavior is observed for the Br case due to the same reason as NiPc-MOF (Supporting Information).

Although the band gap can be tailored through element substitution, the elements we studied are not enough to reverse the sign of the OSE difference between these two states. In order to realize the topological phase transition, we further apply biaxial strain to the systems, which is known to affect the band gap size based on deformation-potential theory.[35−38] We use ZnPc-MOF as a representative example to carry out this computational experiment. The results are summarized in Figure 4, which show that biaxial tensile/compressive strain increases/decreases the lower band gap (Δ_1) between middle band and the lower Dirac band. At the critical compressive strain (3.6%, Figure 4b), the gap Δ_1 closes, leading to a triple degeneracy at the M point. With larger compressive strain, the system remains semimetallic, and it opens the upper gap (Δ_2) between the top Dirac and the middle band (Figure 4c), which further confirms the Lieb lattice nature. The evolution of the gap sizes as a function of external strain is summarized in Figure 4a. There is always one gap that is closed with the other gap showing nearly linear dependence on the external strain before and after the critical strain.

To confirm that the system with closed gap Δ_1 upon compressive strain is indeed in a topological phase, we further calculated the strained system by turning on the SOC interaction. The double degeneracy at the M point is lifted due to the SOC effect, indicating its topological feature. The SOC gap is approximately 3 meV because of the relatively small SOC strength of the ZnPc-MOF (Supporting Information). We fitted the band structure with the TB Hamiltonian based on the maximally localized Wannier function using the Wannier90 package, which agrees very well with our DFT results. Further calculations of the edge state based on the fitted TB Hamiltonian with a semi-infinite structure using Green's function show clearly the nontrivial topological edge state similar as in Figure 1d,f. The spin Chern number and spin Berry curvature results all confirm the system to be a topological insulator. Usually spin Chern number is not well-defined in the presence of SOC, so as a cross check, we also calculated its Z2 number based on Fu-Kane formalism for a spatial inversion symmetric system,[39] which further confirms its topological insulator phase (Supporting Information).

Beside nonmagnetic systems, we further studied CuPc-MOF as one example for magnetic systems. The Cu ion ($3d^{10}4s^1$) donates two electrons to the Pc ligand, leading to a $3d^9$ electronic configuration of Cu^{2+}. Given the local crystal field splitting, the highest d orbital ($d_{x^2-y^2}$) is half-filled with one localized spin ($S = 1/2$). It further couples to the itinerant π electrons, which could possibly lead to more exotic states. To evaluate this idea, we performed a spin-polarized DFT calculation with on-site U correction to properly treat the localized d electrons. Our LDA+U ($U = 4$ eV, $J = 0.9$ eV) calculation shows clearly isolated spin-up and spin-down d bands separated by the Fermi level, as shown in Figure 5a, consistent with the physical picture of localized $S = 1/2$ spins. Different U values are tested, which merely modifies the gap size between the spin-up and spin-down d bands and does not affect the band topology (Supporting Information).

Interestingly, we notice that the Lieb(π)-bands are also spin polarized with two spins shifting in the same direction as the Cu local spins, indicating a ferromagnetic interaction between itinerant π electrons and localized d spins. Given the topological phase transition in nonmagnetic MPc-MOFs, we anticipate that more interesting states would evolve when applying strain to CuPc-MOF. Therefore, we further applied biaxial strain to the CuPc-MOF without considering the SOC effect, for which case the two spins can be treated independently. As summarized in Figure 5b, the evolution of lower band gap (Δ_1) as a function of external strain for two spins is similar as the one for nonmagnetic systems, confirming that the Lieb feature remains robust even for magnetic systems. Because of the spin splitting of the π bands, the critical strain to close the gap Δ_1 becomes different for the two spin channels, which yields several exotic topological phases. Without external strain, the system is in an intrinsic magnetic insulating state (Figure 5a,c). With increasing compressive strain, the spin up band closes first while the spin down state remains gapped, leading to a magnetic semimetal state (Figure 5d) that becomes a Chern insulator when the SOC effect is considered (Supporting Information). While further increasing the compressive strain, the gap of both spins closes, giving rise to a "quasi-semimetal" state (Figure 5e) that potentially leads

Table 2. Band Gap for ZnPc-MOFs with H, F, Cl, and Br

materials	ZnPc-MOF(H)	ZnPc-MOF(F)	ZnPc-MOF(Cl)	ZnPc-MOF(Br)
electronegativity	2.1	4.0	3.0	2.8
band gap (eV)	0.291	0.111	0.134	0.057

https://dx.doi.org/10.1021/acs.nanolett.9b05242
Nano Lett. 2020, 20, 1959−1966

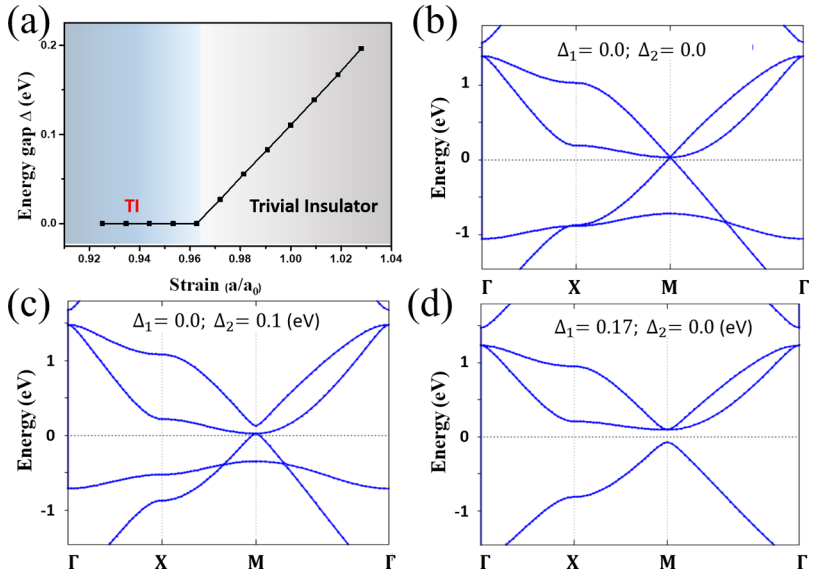

Figure 4. Band structures of ZnPc-MOF under the biaxial strain effect. (a) Evolution of lower band gaps, Δ_1, as a function of external strain. (b–d) Band structure of ZnPc-MOF under 3.8% compressive strain, 6% compressive strain, and 2% tensile strain, respectively.

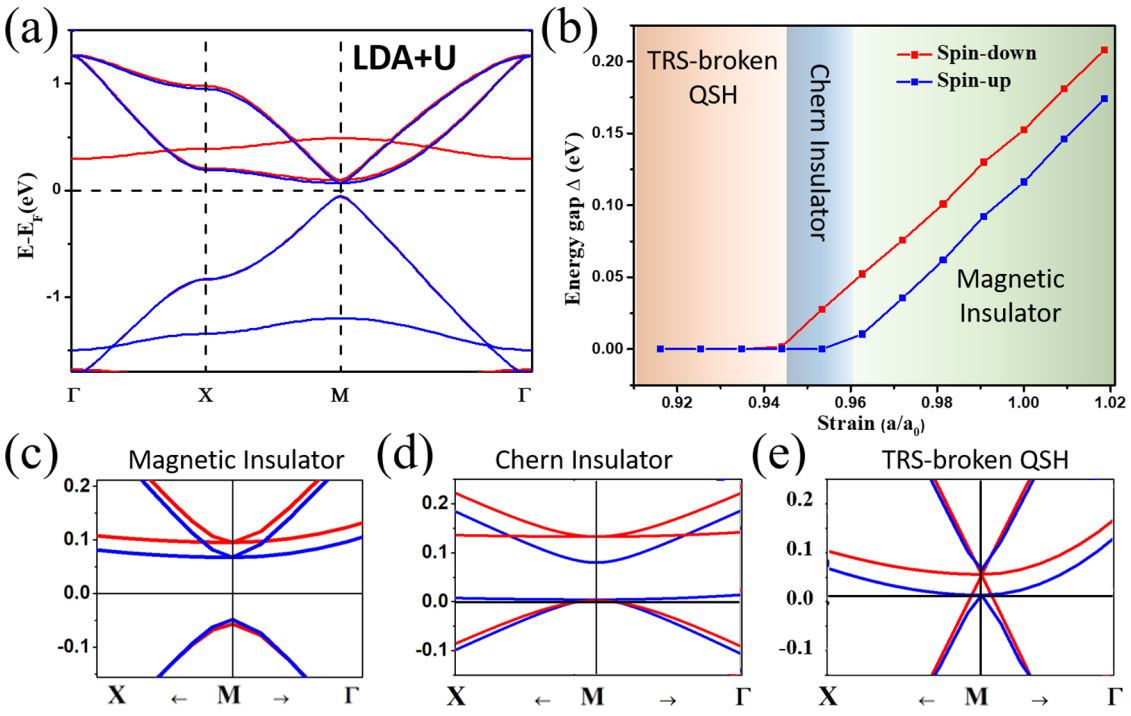

Figure 5. Band structures of the CuPc-MOF crystal under the biaxial strain effect. (a) Band structure of intrinsic CuPc-MOF without external strain. (b) Evolution of topological phases as a function of external strain with the change of lower band gap, Δ_1, for both spins. (c–e) Enlarged band structure around the Fermi level near the M point for the trivial magnetic insulator, Chern insulator, and time-reversal symmetry broken quantum spin Hall state, respectively. Blue/red lines and dots correspond to spin up/down, respectively.

to a time-reversal symmetry broken quantum spin Hall state (TQSH)[40] when considering the SOC effect. However, we note that the TQSH usually requires weak interaction and disorder, which may be difficult to realize in our proposed system (Supporting Information).

It is important to mention that the MPc-based MOFs have already been grown on various metal substrates.[32] The corresponding STM results already show implicitly the Lieb-lattice feature, as we illustrated above in Figure 2a. It is possible to observe the proposed topological phase transition by introducing strain to thin films. This can be experimentally achieved through several approaches, e.g., epitaxial growth, using deformation of flexible substrate, taking advantage of the piezoelectric substrate, or chemical doping and adsorption.[35]

In summary, combining tight-binding simulations and first-principles calculations, we have identified that the phthalocyanine-based MOFs belong to the long-sought-after Lieb-lattice materials with a nonideal Lieb band structure. More interestingly, we establish the basic physical principles to achieve topological states in the Lieb lattice, which has been further applied in real materials of MPc-MOFs through experimentally feasible topological band engineering, i.e.,

https://dx.doi.org/10.1021/acs.nanolett.9b05242
Nano Lett. 2020, 20, 1959–1966

chemical substitution and/or physical strain engineering. Our theoretical discovery substantially enriches the physics of MPc compounds and could potentially lead to their new applications. We hope our work will motivate the experimental search for the Lieb-lattice-based topological materials, which may also be further extended to MOFs/COFs with different structures.

■ ASSOCIATED CONTENT

Supporting Information

The Supporting Information is available free of charge at https://pubs.acs.org/doi/10.1021/acs.nanolett.9b05242.

Additional details on computations; tight-binding modeling; topological characterization; time-reversal symmetry broken QSH effect; LDA and LDA+U calculations of magnetic CuPc-MOF; and additional figures (PDF)

■ AUTHOR INFORMATION

Corresponding Authors

Feng Liu − *Department of Materials Science & Engineering, University of Utah, Salt Lake City, Utah 84112, United States;* orcid.org/0000-0002-3701-8058; Email: fliu@eng.utah.edu

Tony Low − *Department of Electrical & Computer Engineering, University of Minnesota, Minneapolis, Minnesota 55455, United States;* orcid.org/0000-0002-5759-5899; Email: tlow@umn.edu

Authors

Wei Jiang − *Department of Electrical & Computer Engineering, University of Minnesota, Minneapolis, Minnesota 55455, United States;* orcid.org/0000-0001-6167-1156

Shunhong Zhang − *International Center for Quantum Design of Functional Materials (ICQD), Hefei National Laboratory for Physical Sciences at Microscale, and CAS Center For Excellence in Quantum Information and Quantum Physics, University of Science and Technology of China, Hefei, Anhui 230026, China;* orcid.org/0000-0003-2120-4574

Zhengfei Wang − *Hefei National Laboratory for Physical Sciences at the Microscale, University of Science and Technology of China, Hefei, Anhui 230026, China;* orcid.org/0000-0002-0788-9725

Complete contact information is available at: https://pubs.acs.org/10.1021/acs.nanolett.9b05242

Notes

The authors declare no competing financial interest.

■ ACKNOWLEDGMENTS

This project is partly supported by U.S. DOE-BES (Grant DE-FG02-04ER46148). W.J. and T.L. acknowledge the support from SMART, one of seven centers of nCORE, a Semiconductor Research Corporation program, sponsored by National Institute of Standards and Technology (NIST). S.Z. acknowledges the support from NSFC under Grant 11774196. Z.W. acknowledges the support from NSFC (Grants 11774325 and 21603210), National Key Research and Development Program of China (Grant 2017YFA0204904), and Fundamental Research Funds for the Central Universities. Computations of this work were supported by MSI of University of Minnesota and CHPC at University of Utah.

■ REFERENCES

(1) Lieb, E. H. Two theorems on the Hubbard model. *Phys. Rev. Lett.* **1989**, *62*, 1201−1204.

(2) Miyahara, S.; Kusuta, S.; Furukawa, N. BCS theory on a flat band lattice. *Phys. C* **2007**, *460*−*462*, 1145−1146.

(3) Beugeling, W.; Everts, J. C.; Morais Smith, C. Topological phase transitions driven by next-nearest-neighbor hopping in two-dimensional lattices. *Phys. Rev. B: Condens. Matter Mater. Phys.* **2012**, *86*, 195129.

(4) Jiang, W.; Huang, H.; Liu, F. A Lieb-like lattice in a covalent-organic framework and its Stoner ferromagnetism. *Nat. Commun.* **2019**, *10*, 2207.

(5) Ozawa, H.; Taie, S.; Ichinose, T.; Takahashi, Y. Interaction-Driven Shift and Distortion of a Flat Band in an Optical Lieb Lattice. *Phys. Rev. Lett.* **2017**, *118*, 175301.

(6) Mukherjee, S.; Spracklen, A.; Choudhury, D.; Goldman, N.; Öhberg, P.; Andersson, E.; Thomson, R. R. Observation of a Localized Flat-Band State in a Photonic Lieb Lattice. *Phys. Rev. Lett.* **2015**, *114*, 245504.

(7) Slot, M. R.; Gardenier, T. S.; Jacobse, P. H.; van Miert, G. C. P.; Kempkes, S. N.; Zevenhuizen, S. J. M.; Smith, C. M.; Vanmaekelbergh, D.; Swart, I. Experimental realization and characterization of an electronic Lieb lattice. *Nat. Phys.* **2017**, *13*, 672.

(8) Drost, R.; Ojanen, T.; Harju, A.; Liljeroth, P. Topological states in engineered atomic lattices. *Nat. Phys.* **2017**, *13*, 668.

(9) Jin, E.; Asada, M.; Xu, Q.; Dalapati, S.; Addicoat, M. A.; Brady, M. A.; Xu, H.; Nakamura, T.; Heine, T.; Chen, Q.; Jiang, D. Two-dimensional sp^2 carbon−conjugated covalent organic frameworks. *Science* **2017**, *357*, 673−676.

(10) Cui, B.; Zheng, X.; Wang, J.; Liu, D.; Xie, S.; Huang, B. Realization of Lieb lattice in covalent-organic frameworks with tunable topology and magnetism. *Nat. Commun.* **2020**, *11*, 66.

(11) Liu, J.; Xu, Y.; Wu, J.; Gu, B.-L.; Zhang, S. B.; Duan, W. Manipulating topological phase transition by strain. *Acta Crystallogr., Sect. C: Struct. Chem.* **2014**, *70*, 118−122.

(12) Shi, W.-J.; Liu, J.; Xu, Y.; Xiong, S.-J.; Wu, J.; Duan, W. Converting normal insulators into topological insulators via tuning orbital levels. *Phys. Rev. B: Condens. Matter Mater. Phys.* **2015**, *92*, 205118.

(13) Tsai, W.-F.; Fang, C.; Yao, H.; Hu, J. Interaction-driven topological and nematic phases on the Lieb lattice. *New J. Phys.* **2015**, *17*, 055016.

(14) Chen, R.; Zhou, B. Spin Chern number and topological phase transition on the Lieb lattice with spin-orbit coupling. *Phys. Lett. A* **2017**, *381*, 944−948.

(15) Jiang, W.; Kang, M.; Huang, H.; Xu, H.; Low, T.; Liu, F. Topological band evolution between Lieb and kagome lattices. *Phys. Rev. B: Condens. Matter Mater. Phys.* **2019**, *99*, 125131.

(16) Kambe, T.; Sakamoto, R.; Hoshiko, K.; Takada, K.; Miyachi, M.; Ryu, J.-H.; Sasaki, S.; Kim, J.; Nakazato, K.; Takata, M.; Nishihara, H. Π-Conjugated Nickel Bis(dithiolene) Complex Nanosheet. *J. Am. Chem. Soc.* **2013**, *135*, 2462−2465.

(17) Sheberla, D.; Sun, L.; Blood-Forsythe, M. A.; Er, S.; Wade, C. R.; Brozek, C. K.; Aspuru-Guzik, A.; Dincă, M. High Electrical Conductivity in Ni_3(2,3,6,7,10,11-hexaiminotriphenylene)$_2$, a Semiconducting Metal−Organic Graphene Analogue. *J. Am. Chem. Soc.* **2014**, *136*, 8859−8862.

(18) Jiang, W.; Liu, F. *World Scientific Reference on Spin in Organics*; World Scientific, 2018; Chapter 6, pp 201−224.

(19) Chen, H.; Zhang, S.; Jiang, W.; Zhang, C.; Guo, H.; Liu, Z.; Wang, Z.; Liu, F.; Niu, X. Prediction of two-dimensional nodal-line semimetal in a carbon nitride covalent network. *J. Mater. Chem. A* **2018**, *6*, 11252.

(20) Ni, X.; Jiang, W.; Huang, H.; Jin, K.-H.; Liu, F. Intrinsic quantum anomalous hall effect in a two-dimensional anilato-based lattice. *Nanoscale* **2018**, *10*, 11901.

(21) Jiang, W.; Liu, Z.; Mei, J.-W.; Cui, B.; Liu, F. Dichotomy between frustrated local spins and conjugated electrons in a two-dimensional metal-organic framework. *Nanoscale* **2019**, *11*, 955−961.

(22) Wang, Z. F.; Su, N.; Liu, F. Prediction of a Two-Dimensional Organic Topological Insulator. *Nano Lett.* **2013**, *13*, 2842−2845.
(23) Wang, Z. F.; Liu, Z.; Liu, F. Quantum Anomalous Hall Effect in 2D Organic Topological Insulators. *Phys. Rev. Lett.* **2013**, *110*, 196801.
(24) Liu, Z.; Wang, Z.-F.; Mei, J.-W.; Wu, Y.-S.; Liu, F. Flat Chern Band in a Two-Dimensional Organometallic Framework. *Phys. Rev. Lett.* **2013**, *110*, 106804.
(25) Su, N.; Jiang, W.; Wang, Z.; Liu, F. Prediction of large gap flat Chern band in a two-dimensional metal-organic framework. *Appl. Phys. Lett.* **2018**, *112*, 033301.
(26) Thouless, D. J.; Kohmoto, M.; Nightingale, M. P.; den Nijs, M. Quantized Hall Conductance in a Two-Dimensional Periodic Potential. *Phys. Rev. Lett.* **1982**, *49*, 405−408.
(27) Yao, Y.; Kleinman, L.; MacDonald, A. H.; Sinova, J.; Jungwirth, T.; Wang, D.-s.; Wang, E.; Niu, Q. First Principles Calculation of Anomalous Hall Conductivity in Ferromagnetic bcc Fe. *Phys. Rev. Lett.* **2004**, *92*, 037204.
(28) de la Torre, G.; Vazquez, P.; Agullo-Lopez, F.; Torres, T. Role of Structural Factors in the Nonlinear Optical Properties of Phthalocyanines and Related Compounds. *Chem. Rev.* **2004**, *104*, 3723−3750.
(29) Brede, J.; Atodiresei, N.; Kuck, S.; Lazić, P.; Caciuc, V.; Morikawa, Y.; Hoffmann, G.; Blügel, S.; Wiesendanger, R. Spin- and Energy-Dependent Tunneling through a Single Molecule with Intramolecular Spatial Resolution. *Phys. Rev. Lett.* **2010**, *105*, 047204.
(30) Atodiresei, N.; Brede, J.; Lazić, P.; Caciuc, V.; Hoffmann, G.; Wiesendanger, R.; Blügel, S. Design of the Local Spin Polarization at the Organic-Ferromagnetic Interface. *Phys. Rev. Lett.* **2010**, *105*, 066601.
(31) Sanvito, S. Molecular spintronics. *Chem. Soc. Rev.* **2011**, *40*, 3336−3355.
(32) Abel, M.; Clair, S.; Ourdjini, O.; Mossoyan, M.; Porte, L. Single Layer of Polymeric Fe-Phthalocyanine: An Organometallic Sheet on Metal and Thin Insulating Film. *J. Am. Chem. Soc.* **2011**, *133*, 1203−1205.
(33) Zhou, J.; Sun, Q. Magnetism of Phthalocyanine-Based Organometallic Single Porous Sheet. *J. Am. Chem. Soc.* **2011**, *133*, 15113−15119.
(34) Zhou, J.; Wang, Q.; Sun, Q.; Kawazoe, Y.; Jena, P. Strain-Induced Spin Crossover in Phthalocyanine-Based Organometallic Sheets. *J. Phys. Chem. Lett.* **2012**, *3*, 3109−3114.
(35) Deng, S.; Sumant, A. V.; Berry, V. Strain engineering in two-dimensional nanomaterials beyond graphene. *Nano Today* **2018**, *22*, 14−35.
(36) Liu, Z.; Wu, J.; Duan, W.; Lagally, M. G.; Liu, F. Electronic Phase Diagram of Single-Element Silicon "Strain" Superlattices. *Phys. Rev. Lett.* **2010**, *105*, 016802.
(37) Zhou, M.; Liu, Z.; Wang, Z.; Bai, Z.; Feng, Y.; Lagally, M. G.; Liu, F. Strain-Engineered Surface Transport in Si(001): Complete Isolation of the Surface State via Tensile Strain. *Phys. Rev. Lett.* **2013**, *111*, 246801.
(38) Si, C.; Sun, Z.; Liu, F. Strain engineering of graphene: a review. *Nanoscale* **2016**, *8*, 3207−3217.
(39) Fu, L.; Kane, C. L. Topological insulators with inversion symmetry. *Phys. Rev. B: Condens. Matter Mater. Phys.* **2007**, *76*, 045302.
(40) Yang, Y.; Xu, Z.; Sheng, L.; Wang, B.; Xing, D. Y.; Sheng, D. N. Time-Reversal-Symmetry-Broken Quantum Spin Hall Effect. *Phys. Rev. Lett.* **2011**, *107*, 066602.

https://dx.doi.org/10.1021/acs.nanolett.9b05242
Nano Lett. 2020, 20, 1959−1966